International Journal of Mechanical, Industrial and Aerospace Sciences
ISSN: 2517-9950
Vol:7, No:12, 2013

Development of Underactuated Robot Hand Using Cross Section Deformation Spring

Naoki Saito, Daisuke Kon, Toshiyuki Sato

***Abstract*—**This paper describes an underactuated robot hand operated by low-power actuators. It can grasp objects of various shapes using easy operations. This hand is suitable for use as a lightweight prosthetic hand that can grasp various objects using few input channels. To realize operations using a low-power actuator, a cross section deformation spring is proposed. The design procedure of the underactuated robot finger is proposed to realize an adaptive grasping movement. The validity of this mechanism and design procedure are confirmed through an object grasping experiment. Results demonstrate the effectiveness of across section deformation spring in reducing the actuator power. Moreover, adaptive grasping movement is realized by an easy operation.

***Keywords*—**Robot hand, Underactuated mechanism, Cross section deformation spring, Prosthetic hand.

I. Introduction

OUR study goal is the development of a lightweight, dexterous prosthetic hand that can perform various tasks similarly to a human hand. The prosthetic hand must operate with few input signals because of its myoelectric interface. It must also be lightweight because it is installed at the tip of an arm [1]. Many prosthetic hands have been developed in previous studies [2], [3].

A robot hand with an underactuated mechanism for a robot finger has been proposed [4], [5] considering prosthetic hand specifications. The underactuated mechanism has more degrees of freedom than the number of input channels. Therefore, the underactuated mechanism satisfies the requested prosthetic hand specifications. The underactuated robot finger can determine an object grasping posture automatically according to a contact object using appropriate force balancing [6].

These underactuated robot fingers using a spring for expansion operations are divided roughly into a link-transmission type and a tendon-driven type. These differ in their resultant grasping force. The tendon-driven type is suitable for providing precise and sensitive movements such as a pinching operation [7].

For these, the underactuated robot hand is proposed, with an antagonistic mechanism consisting of a tendon and spring. Reportedly, such a robot hand can realize six fundamental grasping operations of a human hand [8].

However, grasping posture and grasping force are important to conduct an object grasping task. Especially, an appropriately determined grasping force is an important factor to maintain a grasping posture. A conventional antagonistic driven mechanism consists of a tendon and a spring [9]. Its joint extension torque increases concomitantly with increasing flexion angle. For that reason, strong tension is necessary to maintain a grasping posture. It is difficult to produce a strong grasping force using this joint mechanism. Extension torque of the joint of this finger is necessary to extend the robot finger against gravity, and to be balanced with tension of the tendon.

However, in dynamics, it is not necessary to make the extension torque increase concomitantly with the increase of the joint angle. Therefore, it is possible to improve the relation of the extension torque and the joint angle. A robot hand that can readily produce a strong grasping force while maintaining a grasping posture can be developed from generation of an extension torque that is as small as possible.

For this reason, in this study, we propose a spring element of a new type, a cross section deformation spring (CSDS), from which extension torque is generated without being dependent on a joint angle. The CSDS effectiveness at decreasing tension of a flexional tendon was confirmed through evaluation of the prototype underactuated robot finger. Furthermore, we suggest the possibility of realizing a robot hand of reduced weight, like a prosthetic hand, through an object grasping experiment.

II. Cross Section Deformation Spring

The CSDS proposed in this study, as presented in Fig. 1, is made of an elastic tube, a part of which is cut off to a triangle. This CSDS bends the cutoff part as a flexural center. Here, as presented in Fig. 2, the cross-section surface shape at the part of bending deformation changes from an arc shape to a flat shape. For this deformation, the moment of inertia of the area changes depending on the bending angle. Therefore, the CSDS has nonlinearity characteristic to a bending angle.

Fig. 1 Cross section deformation spring (CSDS)

In this study, the nonlinear characteristic is confirmed experimentally. Here, the elastic tube material, the cut off part size, outer diameter, and the elastic tube thickness are regarded as design parameters. We discuss CSDS spring characteristics when the parameters are changed. As depicted in Fig. 3, the cutoff part size is defined as the percentage of the cutoff depth:

Naoki Saito is with Akita Prefectural University, Akita, Japan (e-mail: naoki_saito@akita-pu.ac.jp).
Daisuke Kon is with the Graduate School of Akita Prefectural University, Akita, Japan (e-mail: M14A007@akita-pu.ac.jp).
Toshiyuki Sato is with Akita Prefectural University, Akita, Japan (e-mail: tsatoh@akita-pu.ac.jp).

the distance from the outer surface of the elastic tube to the vertical angle of the triangular cutoff part to the outer diameter of the elastic tube.

Fig. 2 Deformation of the CSDS during bending

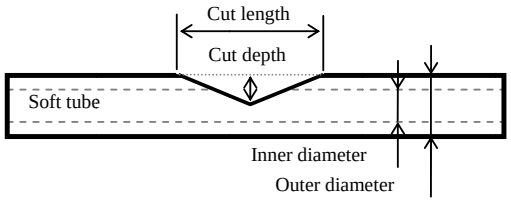

Fig. 3 Line drawing of CSDS

First, we discuss the differences of spring characteristics attributable to the elastic tube material. In this study, a polyurethane (PU) tube and a polypropylene (PP) tube were tested. Their Young's moduli were, respectively0.7 GPa and 1.1 GPa. The CSDS made of PP is slightly harder than the PUs. The cutoff part size is 30%.

The relation of extension torque and bending angle of each CSDS is portrayed in Fig. 4. Both results show that the extension torque increases linearly with increasing bending angle until it reaches 40 deg. Thereafter, the extension torque decreases gently or remains constant. It increases again from near 120 deg. Furthermore, overall, the PP result is greater than the PU result. This is probably true because the Young's modulus of PP is greater than that of other one. However, the qualitative tendency is almost identical. Based on these results, it turns out that the elastic tube material affects the amount of extension torque.

Next, we discuss the relation between the extension torque and the cutoff part size. Here, the extension torque result obtained when the experimental condition is that an outer diameter is 6mm, a material is PU, and the cutoff part size is changed from 30% to 70%, as presented in Fig. 5.

This result confirmed that the extension torque decreases concomitantly with increasing cut off part size. Moreover, it the qualitative tendency changes by changing the cutoff part size. If the cutoff part is small, then the extension torque decreases when the bending angle becomes greater than 40 deg. Thereafter, it increases again. However, if the cutoff part is big, then the tendency of extension torque reduction disappears.

That tendency is believed to derive from the relation of the cutoff part size and the form of the cross section surface of the flexural center. If the cutoff part is small, then the arc in the cross section surface before bending is long. Therefore, the moment of inertia of the area becomes high, and high extension torque is generated. Subsequently the part of the flexural center gradually becomes a flat plate. It becomes easy to bend. Therefore, it is considered that the extension torque decreases.

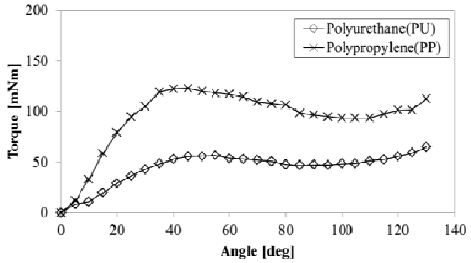

Fig. 4 Relation between bending angle and torque

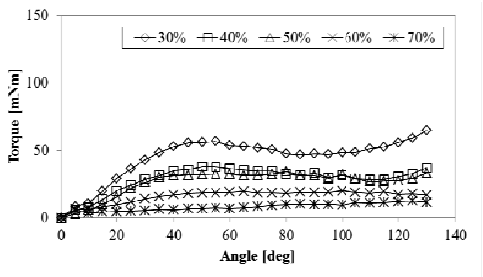

Fig. 5 Characteristic of CSDS made of PU d=6 mm

When the cutoff part becomes large, the arc in the cross section surface is short. It is an almost flat plate before bending. Therefore, the output torque is small. It shows a qualitative tendency resembling that of a linear spring because the cross section surface does not deform to any great extent.

In the case of a tube of PP, the tendency is the same. It is inferred that this tendency is similar for other materials.

This result confirmed that the cutoff part size affects not only the amount of extension torque; it also affects the quantitative tendency of output characteristics.

Here, we discuss the change of extension torque depending on the elastic tube outer diameter and thickness. As an example of an experimental condition, the PU material and outer diameters of 6mm, 8mm, and 10mm were chosen. The elastic tube thickness is decided by the standard respectively as 1.0mm, 1.5mm, and 1.75mm. The cutoff part size is unified as 50% with each diameter. The relation between the bending angle and extension torque in this experimental condition is portrayed in Fig. 6.

This result demonstrates that the tendency of extension torque increases concomitantly with increasing outer diameter. In addition, the characteristic changes because of a difference in the elastic tube material when the bending angle is greater than 40 deg. For PU, the extension torque increases gently or remains constant, but in the case of PP, the extension torque decreases first and increases gradually. This qualitative tendency does not change to a great degree even if the elastic tube outer diameter is changed, but it depends on the material.

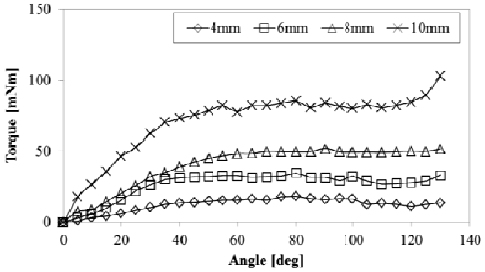

Fig. 6 Characteristics of CSDS made of PU (Depth 50%)

Based on this result, the CSDS was confirmed to have a nonlinear torque characteristic as a main characteristic. The extension torque increases concomitantly with increasing Young's modulus, outer diameter or thickness, and with decreasing size of the cutoff part.

III. Design of a Robot Finger Incorporating CSDS

A. Outline of the Robot Finger

An outline of a proposed underactuated robot finger is portrayed in Fig. 7. This robot finger has three joints in one finger, with each joint extended by a spring.

This finger has one flexural tendon. Each joint of the underactuated finger is flexed by pulling this tendon. Furthermore, the angle of each joint is decided automatically along an object shape.

For this study, the robot finger flexing movement is designed as follows. First, only a metacarpophalangeal joint (MP joint) is flexed completely. Next, a proximal interphalangeal joint (PIP joint) is flexed. After the PIP joint is flexed completely, a distal interphalangeal joint (DIP joint) is flexed. We designate this movement as an adaptive grasping movement. The design procedure of a robot finger to achieve this movement is described in the following section.

B. Robot Finger Design for an Adaptive Grasping Movement

An adaptive grasping movement is achieved by designing the robot finger structure considering these quence of flexion of each joint. For each joint, the extension torque generated by an elastic element, torque generated by mass of the robot finger and gravity, and flexion torque generated by an actuator are denoted respectively as τE_i,τG_i, and τF_i. Here, index i is an identifier of each joint, such as MP, PIP, and DIP.

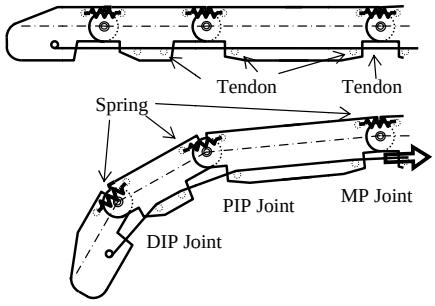

Fig. 7 Basic mechanism of the proposed robot finger

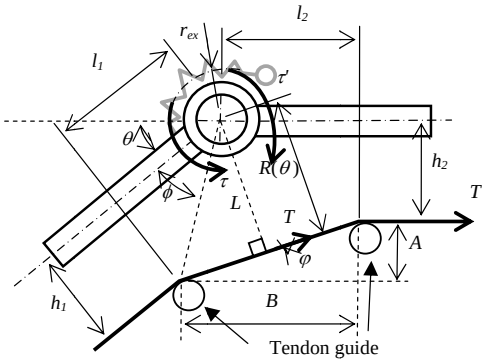

Fig. 8 Geometrical model of joint of the robot finger

If an extension torque is generated by an elastic element such as a spring, then the postures in which a robot finger is maintained horizontally are the conditions requiring the greatest torque. Moreover, the grasping movement must be achieved irrespective of the robot hand posture. Therefore, it is necessary to consider the flexural direction of the robot finger not only from the horizontal direction downward, but also from the horizontal direction upward.

These conditions can be expressed by the direction and magnitude of extension torque, the torque resulting from gravity, and flexural torque. The relation of extension torque on each joint considering achievement of the adaptive grasping movement is expressed as

$$\tau E_{DIP} > \tau E_{PIP} > \tau E_{MP} > \tau G_{MP} \tag{1}$$

Next, we derive the flexural torque. The flexural torque changes because of the joint flexural angle and tension generated by an actuator. Fig. 8 shows the joint torque model, which includes flexion torque, extension torque, and relevant parameters of these torques. Here, the flexural torque of each joint is derived by application of this model to each joint. The flexural torque of each joint is expressed as follows using a tension of flexural tendon, which is denoted as T:

$$\tau F_i = R_i(\theta_i)T \tag{2}$$

$$R_i(\theta_i) = \sqrt{{l_{1i}}^2 + {h_{1i}}^2}\sin(\theta_i + \phi_i - \varphi_i) \tag{3}$$

In (2) and (3), index *i* is an identifier of each joint. Although an identifier is attached to a joint angle, an identifier is not attached to tension because each joint is flexed by the tension of one flexural tendon. Angles$\phi_i$and $\varphi_i$are derived respectively from geometrical relations.

Results of prototyping an underactuated robot finger show that the torque resulting from gravity of MP joint $\tau G_{MP}$is 23.0 mNm.

Fig. 9 presents the relation between the joint angle and torque of the CSDS adopted as each joint considering the amount of torque of MP joint. The CSDS was built into each

joint of the completely extended prototype robot finger as it was flexed to 40 deg. Therefore, the flexural range of each CSDS is from 40 deg to 130 deg. By this usage, extension torque generated by the CSDS of MP joint is from 40 mNm to 43 mNm, it is assumed to be constant. Moreover, the extension torque of the PIP joint and the DIP joint when the finger is extended completely are, respectively, 70 mNm and 77 mNm. The torque of these joints decreases to about 55 mNm with increasing joint flexural angle. For the PIP joint and DIP joint, because the extension torque decreases after flexural torque exceeds the maximum extension torque, it is possible to reduce the flexural posture of the finger by smaller flexural torque compared with the mechanism that is extending with a linear elastic element such as a torsion spring.

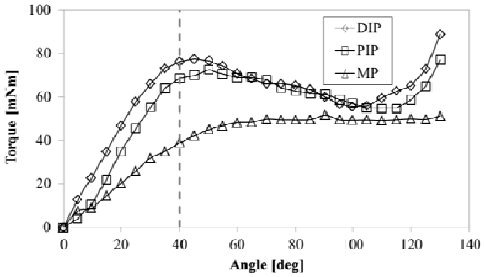

Fig. 9 Characteristic of CSDSs actually incorporated in the robot finger

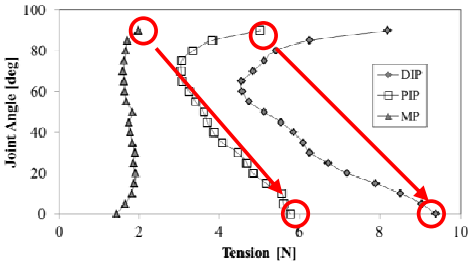

Fig. 10 Simulation result of the relation between pulling tension and each joint angle

Fig. 10 presents calculation results of the relation of tension of a tendon in the designed robot finger and the angle of each joint. The MP joint begins flexion when the tension exceeds 3N. It flexes completely when the tension reaches 3.8N. The PIP joint does not flex when the tension becomes greater than 6N. Therefore, the PIP joint does not flex before the MP joint reaches 90 deg. Subsequently, the PIP joint flexes quickly and reaches 90 deg immediately after the tension becomes greater than 6N.

The DIP joint begins flexing when the tension exceeds 9.5N. The result of this pattern of movement shows that this design procedure can produce an adaptive grasping movement.

In the next section, the validity of this design procedure is confirmed experimentally using the underactuated robot finger. The underactuated joint mechanism using CSDS is evaluated in comparison with the extension mechanism using a commercial torsion spring built into another underactuated robot finger.

IV. Evaluation of the Robot Finger

The prototype robot finger, produced mainly from ABS resin, is presented in Fig. 11. The finger width is almost identical to that of an adult male, with length that is 1.2 times longer than that of an adult male. Tension to a flexural tendon is generated by an air cylinder. The validity of the design procedure for making adaptive grasping movement through a flexing action test was confirmed by this prototype robot finger using CSDS.

A. Flexing Action Test

First, adaptive grasping by the prototype robot finger is checked. In the experiment, the tension which increases 1N at a time is added to the flexural tendon by a pneumatic cylinder. Each joint angle at that time was measured using an image processing program. The robot finger posture is downward in a horizontal direction, upward in a horizontal direction, and upward in a vertical direction. Experimental results of each robot hand posture are, presented respectively in Figs. 12-14.

Fig. 11 Prototype of the robot finger incorporating CSDS

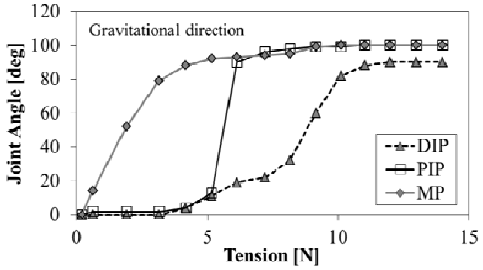

Fig. 12 Experimental result of finger flexion (Gravitational direction)

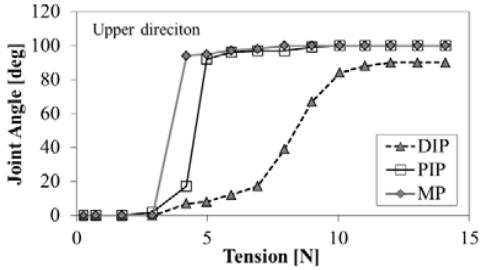

Fig. 13 Experimental result of finger flexion (Upper direction)

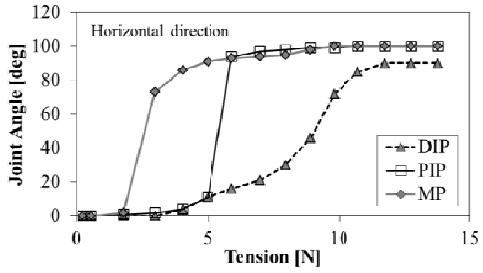

Fig. 14 Experimental result of finger flexion (Horizontal direction)

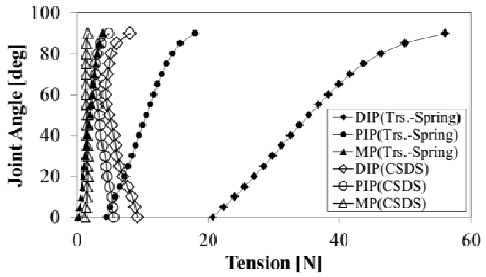

Fig. 15 Relation between pulling tension and each joint angle of the finger using torsional spring and using CSDS

Although the tension at which the joint begins flexing differs, these results show that the turn of flexion of three joints and the timing of flexion of these joints at which one joint begins flexing after the next joint flexes completely are synchronized. Therefore, results confirmed that the adaptive grasping movement is achieved with any posture of the robot finger. Based on these results, the validity of the design procedure considering the balance of each joint torque and joint torque model was confirmed.

B. Advantage of the CSDS

In this section, tension measurements for the mechanism with CSDS and the tension in the mechanism with the commercial torsion spring [8] are compared to examine the advantages of CSDS. Here, adequate torsion springs to a robot finger with specifications that are the same as the prototype robot finger are selected considering the achievement of an adaptive grasping movement. The relation between the angle of each joint and tension of a flexural tendon is simulated. Therefore, the torque resulting from gravity on the MP joint and the flexural torque of all joints generated by the flexural tendon tension areas shown in Fig. 10. Simulation results considering these conditions are presented in Fig. 15, which also shows the result for Fig. 10 for comparison.

This result demonstrates that the robot finger incorporating the CSDS is flexed completely by tension of about 10N. However, tension of about 56N is necessary when a torsion spring is incorporated. Therefore, about 46N of tension of the flexural tendon is decreasing. If it is considered that flexural tendon tension is transformed into both a force for maintaining the grasping posture and a grasping force, then it is easy to generate a great grasping force using CSDS. Based on these results, CSDS is effective as an extension mechanism of an underactuated robot finger.

V. Object Grasping Experiment

The robot hand presented in Fig. 16 was manufactured to confirm the usability of the proposed robot finger in an object grasping task. These five fingers are the same as the robot finger manufactured in previous chapter. The size of the hand, comprising a palm and four fingers except the thumb and palm is 100×270×27mm. This prototype robot hand is 1.2 times longer than that of an adult male. Each finger is flexed by application of pressure to the pneumatic cylinder connected with a flexion tendon. This robot hand can grasp various objects using a simple operation. Therefore, the same pressure is applied simultaneously to five cylinders. We demonstrate an adaptive grasping movement by simple operation of the proposed robot hand. Moreover, we evaluate the distribution of the grasping pressure when the robot hand grasps an object. These results confirmed the usability of the robot hand in the object grasping task.

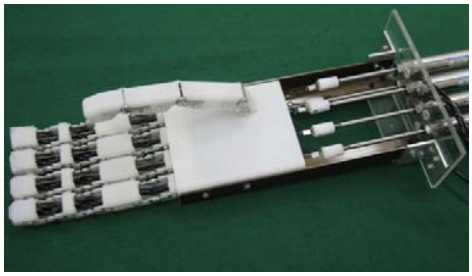

Fig. 16 Appearance of the CSDS robot hand

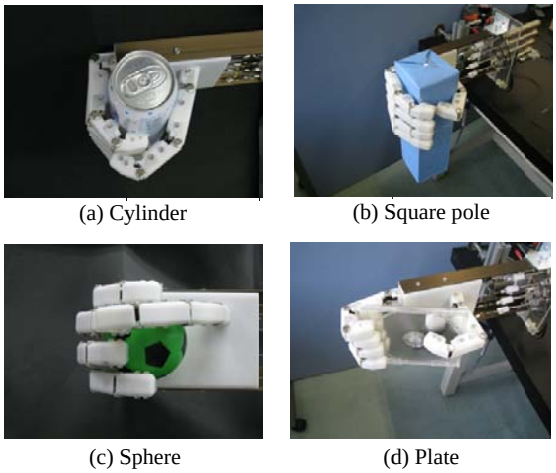

(a) Cylinder (b) Square pole

(c) Sphere (d) Plate

Fig. 17 Experimental result of object grasping

First, we confirmed the achievement of the adaptive grasping movement for a various shaped objects. Experimental results are presented in Fig. 17. In all grasping movements, the supplied pressure of the robot hand is 0.1 MPa. This robot hand can grasp variously shaped objects adaptively. Results show that that the adaptive grasping movement is effective to grasp objects of various shapes.

Next, we assessed the grasping pressure distribution. For this experiment, we used a sheet sensor: a pressure-sensitive conductive coating material applied to the PET film (I-SCAN; Nitta Corp.) for measurement of grasping pressure distribution. This sheet sensor was fixed on the grasping object surface because of the influence on the robot hand joint torque by fixing the sheet sensor on the robot hand surface. In this experiment, the robot hand grasped a 93-mm-diameter cylinder. Flexion tendon tension of 18N was applied simultaneously to all fingers. Next, we discuss the pressure distribution results.

Object grasping and the pressure distribution results of this experiment are presented respectively in Figs. 18 and 19.

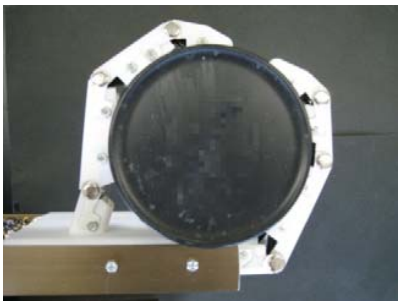

Fig. 18 Appearance of object grasping

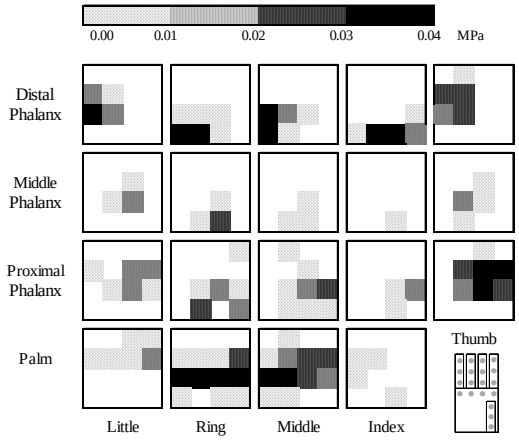

Fig. 19 Distribution of tactile pressure

Contact occurred in all parts of almost all fingers. Each finger link has even contact with the cylindrical object. A tendency was visible by which the contact pressure at the palm and proximal phalanx of the thumb and distal phalanx of all fingers are increasing. The contact pressure at distal phalanx of all fingers increases because the underactuated mechanism of this robot finger generates grasping force by restraining a distal phalanx. Therefore, in a grasping movement, the posture of the middle phalanx and proximal phalanx of the robot finger are decided mostly without generating force.

The contact pressure at the palm and the distal phalanx of index finger and thumb are increased remarkably because the grasping force is generated at the distal phalanx of all fingers. These are balanced by receiving the force at the palm.

Moreover, contact pressure on the proximal phalanx of the thumb increased because this part received contact pressure of the distal phalanx, middle phalanx, and proximal phalanx of the index finger. Originally, the proximal phalanx of the thumb does not generate contact force in adaptive grasping movement. However, contact pressure becomes high. Results suggest that the finger maintains its own posture against the force from the outside.

Contact pressure is acting on the cylindrical object from many directions. These are mutually balanced. This result demonstrates that stable grasping was realized.

These results showed that this robot hand can grasp objects of various shapes stably by easy operation such as application of equal tension to all fingers simultaneously.

VI. Conclusion

As described in this paper, we proposed the underactuated robot hand using a cross section deformation spring for purposes of using the force of an actuator efficiently and grasping various objects through easy operation. The salient results obtained in this study are described below.

1. A cross section deformation spring (CSDS) is proposed as a new spring mechanism. The CSDS has a constant torque characteristic and a torque reduction characteristic. These characteristics depend on the shape of the CSDS cutoff part.
2. Design procedures of the underactuated robot finger using the CSDS were presented. The validity of this design procedure was confirmed experimentally.
3. The CSDS effects were confirmed in simulations. Results show that the tension applied to a flexion tendon of the robot finger using cross section deformation spring is only 18% of the robot finger tension using the torsion spring.
4. The robot hand grasping movement was confirmed experimentally.

The experimentally obtained results and related discussion clarified that this robot hand can grasp objects of various shapes stably through easy operation, giving slight tension to all the robot fingers.

References

[1] R. Crowder, "An anthropomorphic robotic end effector," *Robotics and Autonomous Sys.*vol. 7, pp. 253-268, 1991.
[2] N. Dechev and W. Cleghorn,"Multiple finger, passive adaptive grasp prosthetic hand," *Mech. and Machine Theory.* vol. 36, pp.1157-1173, 2001.
[3] C. Light and P. Chappell, "Development of a lightweight and adaptable multiple-axis hand prosthesis," *Med. Eng. & Phys.* vol. 22, no. 10, pp.679-684, 2000.
[4] H. Yokoi, A. H. Arieta, R. Katoh, W. Yu, I. Watanabe, and M. Maruishi, "Mutual Adaptation in a Prosthetics Application," *Embodied Artificial Intelligence*, pp. 146-159, 2004.
[5] Y. Kamikawa and T. Maeno, "Underactuated Five-Finger Prosthetic Hand Inspired by Grasping Force Distribution of Humans," *Proc. of IEEE/RSJ Int. Conf. on Intel. Rob. and Sys.* pp. 717-722, 2008.
[6] S. Hirose and Y. Umetami, "The development of soft gripper for the versatile robot hand," *Mech. and Machine Theory.* vol. 13, pp. 351-359, 1997.
[7] M.R. Cutkosky, "On grasp choice, grasp models, and the design of hands for manufacturing tasks," *IEEE, Trans. on Rob. and Auto.* vol. 5, no. 3: pp. 269-279, 1989.

[8] S. A. Dally, T. E. Wiste, T. J. Withrow, and M. Goldfarb, "Design of a Multifunctional Anthropomorphic Prosthetic Hand With Extrinsic Actuation," *IEEE/ASME Trans. on Mech.* vol. 14, no. 6, pp. 699-706, 2009.
[9] H. de Visser and J. L. Herder, "Force-directed design of a voluntary closing hand prosthesis," *J. of Rehabili. Res. and Dev.* vol. 37, no. 3, pp. 261-271, 2000.